

Assessing the Global Resilience of Water Quality Sensor Placement Strategies within Water Distribution Systems

Qingzhou Zhang¹, Feifei Zheng², Zoran Kapelan³, Dragan Savic⁴, Guilin He⁵, and Yiyi Ma⁶

¹**Qingzhou Zhang:** Postdoctoral Research Fellow, College of Civil Engineering and Architecture, Zhejiang University, China. wdswater@gmail.com.

²**Feifei Zheng:** Corresponding author, Professor, College of Civil Engineering and Architecture, Zhejiang University, China. feifeizheng@zju.edu.cn. Tel: +86-571-8820-6757. Postal address: A501, Anzhong Building, Zijingang Campus, Zhejiang University, 866 Yuhangtang Rd, Hangzhou, China 310058.

³**Zoran Kapelan,** Professor, Delft University of Technology, Faculty of Civil Engineering and Geosciences, Department of Water Management, Stevinweg 1, 2628 CN Delft, Netherlands. z.kapelan@tudelft.nl

⁴**Dragan Savic:** Chief Executive Officer, KWR Water Research Institute, Dragan.Savic@kwrwater.nl, Professor, Centre for Water Systems, University of Exeter, North Park Road, Exeter, EX4 4QF, United Kingdom.

⁵**Guilin He:** Lectuer, School of Municipal and Environmental Engineering, Shandong Jianzhu University, glhe@zju.edu.cn

⁶**Yiyi Ma:** Assistant Professor, College of Civil Engineering and Architecture, Zhejiang University, China. yiyima@zju.edu.cn

Abstract: Water quality sensors are often spatially distributed in water distribution systems (WDSs) to detect contamination events and monitor quality parameters (e.g., chlorine residual levels), thereby ensuring safety of a WDS. The performance of a water quality sensor placement strategy (WQSPS) is not only affected by sensor spatial deployment that has been extensively analyzed in literature, but also by possible sensor failures that have been rarely explored so far. However, enumerating all possible sensor failure scenarios is computationally infeasible for a WQSPS with a large number of sensors. To this end, this paper proposes an evolutionary algorithm (EA) based method to systematically and efficiently investigate the WQSPS' global resilience considering sensor failures. First, new metrics are developed in the proposed method to assess the global resilience of a WQSPS. This is followed by a proposal of an efficient optimization approach based on an EA to identify the values of global resilience metrics. Finally, the sensors within the WQSPS are ranked to identify their relative importance in maintaining the WQSPS's detection performance. Two real-world WDSs with four WQSPSs for each case study are used to demonstrate the utility of the proposed method. Results show that: (i) compared to the traditional global resilience analysis method, the proposed EA-based approach identifies improved values of global resilience metrics, (ii) the WQSPSs that deploy sensors close to large demand users are overall more resilient in handling sensor failures relative to other design solutions, thus offering important insight to facilitate the selection of WQSPSs, and (iii) sensor rankings based on the global resilience can identify those sensors whose failure would significantly reduce the WQSPS's performance thereby providing guidance to enable effective water quality sensor management and maintenance.

Keywords: Global resilience; Contamination intrusion; Water quality sensor placement strategy; Water distribution system

1. Introduction

A water distribution system (WDS) is a network that is responsible for delivering drinking water produced at treatment plants to end users (Zheng et al., 2016; Qi et al., 2018). Because of a large spatial coverage and complex structures, WDSs are highly vulnerable to intentional or accidental contamination intrusion (Yang and Boccelli 2016; Zheng et al., 2018). A recent intrusion incident was reported in May 2016 in Beijing, China, where a large amount of reclaimed water entered into the WDS due to the misconnection between reclaimed and drinking water supply pipes (ChinaNews, 2016). The event had not been detected for a while and has resulted in severe public health hazard. This highlights the great importance and necessity to efficiently identify contamination intrusion incidents, thereby minimizing the potential impacts of these events (Ostfeld et al., 2004). To achieve this objective, water quality sensors are often placed within the WDSs (i.e., type of sensors and their deployments) to form a contamination early warning system, aimed to ensure potential intrusion events can be detected and a warning can be provided to the public in an efficient manner (Wu and Walski, 2006; Hart and Murray, 2010; Kroll and King 2010; Hu et al., 2017; Soldevila et al., 2018). However, due to the high cost associated with water quality sensors, it is impossible to deploy them at all possible locations in a large WDS (Zhao et al., 2016). This consequently motivates studies to investigate optimal deployment of a limited number of sensors in the WDSs aimed at maximizing their performance in detecting water quality issues (Rathi et al., 2015).

Identifying water quality sensor placement strategies (WQSPS) typically involves formulating an optimization problem (Oliker and Ostfeld, 2014). Over the past decade, a number of different optimization objective functions have been developed to maximize the detection ability of the limited number of water quality sensors. These include the minimization of the detection time

(Ostfeld et al., 2004), the maximization of the detection coverage (Rathi et al., 2015), the minimization of affected users (Aral et al., 2010), the minimization of sensor redundancy (Tinelli et al., 2018), the minimization of the maximum possible influence expressed as the event with the highest consequence (Watson et al., 2009), the minimization of the mean extent of the potential source area and redundant detection (Van, 2014) as well as the minimization of the risk of contamination (Weickgenannt et al 2010). It has been demonstrated that the use of different objective functions can lead to significantly different WQSPSs, and hence it is often difficult to identify a single WQSPS that can ensure all these objectives are optimized (Zheng et al., 2018). To address this issue, the methods of integrating multiple objectives through weighting approaches or simultaneously considering multiple objectives within the optimization framework are adopted to account for the trade-offs between different objectives (He et al., 2018).

In parallel with the development of objective functions, many optimization techniques have been proposed to enable these objective functions to be effectively minimized/maximized (Berry et al., 2005; Bahadur et al., 2003; Hart and Murray, 2010). Among these optimization methods, Evolutionary Algorithms (EAs) have gained in popularity due to their strong search ability as well as their flexibility in linking to water quality simulation models (e.g., EPANET2.0, Ostfeld et al., 2008). The practical applications of EAs to identify optimal WQSPSs are often challenged by their low computational efficiency especially when dealing with large WDSs (Zheng et al., 2017). This is because the EA search mechanisms are stochastically based and hence they need to call continuously the water quality simulation model (that is often computationally expensive) to enable the calculations of objective functions (Hart and Murray, 2010). To overcome this issue, continuous efforts have been made to improve the optimization efficiency with the aid of many techniques, including graph theory (Perelman and Ostfeld, 2011), preconditioning methods (Huang

and Mcbean, 2006; Diao and Rauch, 2013), surrogate models (Bi and Dandy, 2015), data-archive methods (He et al., 2018) and sampling methods (Tinelli et al. 2017).

Given the selected objective function and the optimization algorithm as mentioned above, optimal WQSPSs that have the best overall performance in detecting water quality issues can be identified for the WDS. However, it should be noted that the WQSPS' performance is not only affected by spatial sensor deployment, but can also be substantially influenced by sensor failures (e.g., structural failures and communication failures). Failures of water quality sensors are not uncommon within practical applications, as they can be caused by internal structural failures, measurement errors, or communication failures (Berry et al., 2009). These failures can significantly reduce the performance of the optimal WQSPS that is identified based on the assumption that all water quality sensors can consistently provide accurate measurements (Berry et al., 2009). Therefore, there is a need to consider the resilience during the selection of WQSPSs, thereby ensuring the system performs well not only under normal conditions (perfectly working sensors), but also maintains acceptable functionality levels during unexpected conditions that lead to sensor failures.

Resilience in engineering community is often defined as a system's ability to ensure the continuity and efficiency of its function during and after the failure (Mugume et al., 2015). This concept has now been considered in some engineering domains, such as urban drainage systems (Mugume et al., 2015), water supply systems (Diao et al., 2016; Meng et al., 2018) and wastewater systems (Sweetapple et al., 2019). However, to the best of our knowledge, the WQSPS's resilience that accounts for sensor failures has been rarely investigated so far, and hence there is still a lack of suitable method for resilience quantification. While Preis and Ostfeld (2008) and Berry et al. (2009) have made attempts to consider sensor failures during the selection/assessment of WQSPSs,

they assume a known and fixed failure likelihood for each water quality sensor. However, these approaches only considered a narrow range of possible sensor failures, and hence the results can only represent a limited view of resilience (Mugume et al., 2015). Given that the failure probability of each sensor as well as the total number of failed sensors is actually unknown and unpredictable, it is ideal to explicitly consider all possible failure scenarios, thereby quantifying the global resilience of the WQSPS in coping with possible sensor failures (Butler et al., 2014; Diao et al., 2016). However, enumerating all possible sensor failure scenarios is often computationally infeasible for WQSPSs with a large number of sensors. To this end, this study proposes an EA-based method to investigate the global resilience of WQSPSs considering all sensor failure scenarios.

Rather than quantifying the probability of occurrence of sensor failures, which are highly uncertain, the proposed global resilience evaluation method considers the system performance as a result of sensor failure scenarios irrespective of their occurrence probability (Diao et al., 2016). The specific contributions/novelty of the present study are as follows:

- (i) *The proposal of new metrics to assess the global resilience of WQSPSs under different sensor failure levels (i.e., the number of failed sensors).* In this study, assessment metrics are proposed to measure quantitatively the WQSPS's global resilience under different sensor failure levels, where the impacts of different number of sensor failure scenarios on the WQSPS's ability to detect contamination intrusions are considered, irrespective of their occurrence probability.
- (ii) *The development of a novel EA-based optimization approach to identify the values of the global resilience metrics for different sensor failure levels.* To demonstrate the utility of the proposed EA-based method (EAM), its performance is compared with the traditional global

resilience analysis (TGRA) approach (Diao et al., 2016) in capturing the impact extents of the failure scenarios.

- (iii) *Identification of the relative importance of the sensors in maintaining the WQSPS's detection performance based on the global resilience metric values.* This also helps improving knowledge of the underlying system properties of the WQSPSs as well as offering important guidance for the management and maintenance of water quality sensor systems.

This paper is organized as follows. The proposed methodology is described in Section 2, where the definition of the global resilience metrics and the proposed EAM are presented. This is followed by the descriptions of the case studies considered in Section 3, and results and discussions in Section 4. Finally, the conclusion section (Section 5) shows the main observations and implications of this paper.

2. Methodology

2.1 Global resilience metrics for WQSPSs

2.1.1 Global resilience metrics definition

The proposed global resilience metrics are characterized by the consumed contaminated water of the WDS during the contamination events. A more resilient WQSPS indicates its better ability in detecting contamination events under different sensor failure levels and accordingly less contaminated water would be consumed. The (percentage) functionality loss of the WQSPS under different sensor failure levels (L) can be mathematically described as

$$FL(S_L^k, E_i, t) = \frac{\sum_{j=1}^N Q_j(S_L^k, E_i, t)}{\sum_{j=1}^N DQ_j(t)} \quad (1)$$

where $FL(S_L^k, E_i, t)$ is the proportion of contaminated water that has been consumed relative to the total consumed water of the entire WDS under the intrusion event E_i ($i=1,2,\dots,M$, M is the total number of intrusion events) at time t for the sensor failure scenario k ($k=1,2,\dots,K$, K is the total number of sensor failure scenarios) with L failed sensors (referred as S_L^k); $Q_j(S_L^k, E_i, t)$ is the contaminated water that has been consumed at node j ($j=1,2,\dots,N$, N is the total number of nodes with demand users) and $DQ_j(t)$ is the total water demands required by node j .

Figure 1 further illustrates the proposed formulation of the global WQSPS resilience. As shown in this figure, the black solid curve line represents the dynamic behavior of the functionality level of the WDS (i.e., $1 - FL(S_L^k, E_i, t)$) associated with the WQSPS over time for a given contamination event E_i starting at time t_i^s and a given sensor failure scenario. It is seen that the functionality level of the WDS before the occurrence of the contamination event is 100%. This functionality level value consistently declines for the duration of the contamination event until this event is detected by the WQSPS within the WDS at time t_i^d . The shaded region A between t_i^s and t_i^d is the total functionality losses of the WDS (i.e., the consumed contaminated water) during this time period as indicated in Figure 1. If this contamination event cannot be detected by the WQSPS, the functionality level would gradually increase after a period of reduction as indicated by the black dotted line in Figure 1. This is because the contamination intrusion, especially the intentional contamination injections, often lasts a limited time period (e.g., 1 to 2 hours, see

Ostfeld et al., 2016 and He et al., 2018) and hence the functionality level of the WQS can improve as the contaminated water is consumed over time. For this case, the total functionality losses of the WDS are the shaded region A+B above the black solid and dotted curve lines in Figure 1.

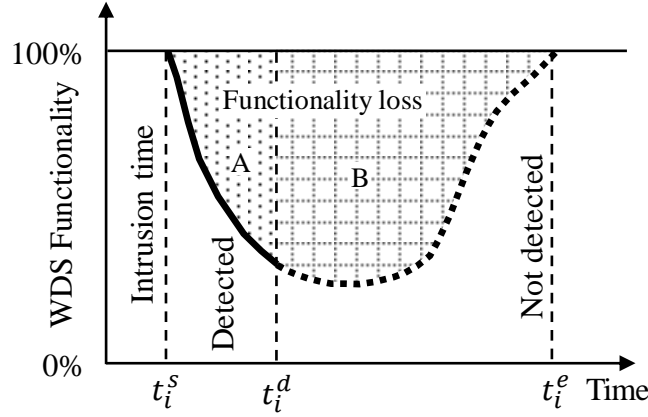


Fig. 1. Illustration of the dynamic behavior of the WDS's functionality level over time for a given contamination event and a given sensor failure scenario.

For all M contamination events, the average of functionality levels (in percentage) of the WQSPS is developed as shown below

$$f(S_L^k) = \frac{1}{M} \sum_{i=1}^M \left[1 - \frac{1}{(t_i^e - t_i^s)} \int_{t_i^s}^{T_i} FL(S_L^k, E_i, t) dt \right] \quad (2)$$

$$T_i = \begin{cases} t_i^d, & E_i \text{ is detected} \\ t_i^e, & E_i \text{ can not be detected} \end{cases} \quad (3)$$

where $f(S_L^k)$ is the average of functionality levels (in percentage) of the WQSPS across M contamination events for the sensor failure scenario S_L^k ; $\int_{t_i^s}^{T_i} FL(S_L^k, E_i, t) dt$ is the accumulative

functionality losses for the intrusion event starting at time t_i^s and ending at time T_i , and this value is normalized between 0 and 1 through dividing it by the time difference between t_i^e and t_i^s (i.e., $t_i^e - t_i^s$), where t_i^e is the time at which all the contaminated water within the WDS has been consumed without detected by the water quality sensors. As shown in Equation (3), if a contamination event E_i can be detected by any sensors with normal functionalities, T_i equals to t_i^d which is the time at which any of the sensors first detects this event. If the contamination event cannot be detected, T_i is set to be t_i^e which is the time when all the contaminated water have been consumed by customers.

The rationale behind the use of the Equations (1) and (2) to represent the resilience of the WQSPS is that this formulation is able to simultaneously consider the impacts of sensor failures on the detection coverage and the time used to detect the contamination events, and the global resilience values are accordingly estimated when all possible failure scenarios are considered. In this study, three metrics are proposed to enable the global resilience assessment under a certain sensor failure level (L), which can be defined as follows

$$R_{\max}(L) = \max\{f(\mathbf{S}_L)\} \quad (4)$$

$$R_{\min}(L) = \min\{f(\mathbf{S}_L)\} \quad (5)$$

$$R_{\text{mean}}(L) = \frac{1}{K} \sum f(\mathbf{S}_L) \quad (6)$$

where $R_{\min}(L)$, $R_{\max}(L)$, $R_{\text{mean}}(L)$ are the minimum, maximum and mean of global resilience values respectively for a given sensor failure level L ; $f(\mathbf{S}_L)$ is the performance level function

that is used to represent the resilience values of the WQSPSs and $\mathbf{S}_L = [S_L^1, S_L^2, \dots, S_L^K]^T$ is the set that contains all possible scenarios with L failed sensors where K is the total number of sensor failure scenarios; the resilience value of each scenario S_L^k is computed using Equation (1).

Based on the definition of the global resilience metrics in Equations (1-6), a more resilient WQSPS would possess overall lower total functionality losses of the WDS (the shaded region in Figure 1) when their sensors fail (considering different failure levels). It is noted that Figure 1 only illustrates the dynamic behavior of the functionality level variations of the WDS over time for one contamination event under a given sensor failure scenario. To enable the identification of the global resilience, a large number of contamination events (M) and all possible sensor failure scenarios (\mathbf{S}_L) need to be considered. The global resilience as proposed in this paper (Equations 1-6) can have a value between 0 and 1, with a larger value representing that the WQSPS being considered is more resilient as it can maintain acceptable detection performance during unexpected conditions that lead to sensor failures. Two important assumptions are made in the proposed global resilience metrics following Ostfeld et al. (2008). These are that: (i) the functionality level of the WDS is not further reduced once the contamination event has been detected (the A shaded region in Figure 1) by the water quality sensors as all users can be quickly notified/warned to avoid consuming contaminated water, and (ii) the time period of the contamination injections is limited as this is often the case for many intentional/accidental intrusion events (Diao et al., 2016).

2.1.2 Sensor failure scenarios

As shown in Equations (4-6), S_L includes all possible failure scenarios for a given failure level L , leading to a total of $C(TL, L)$ failure scenarios (TL is the total number of sensors within the WDS). Taking a WDS with four water quality sensors ($TL=4$) as an example, the total number of scenarios involving a random failure of a single sensor is four ($C(4,1)=4$) as shown in Fig. 2. For failure levels of $L=2, 3$ and 4 , the total number of scenarios are six, four and one respectively (see Fig. 2). Therefore, for this small WQSPS, the total number of failure scenarios is 15.

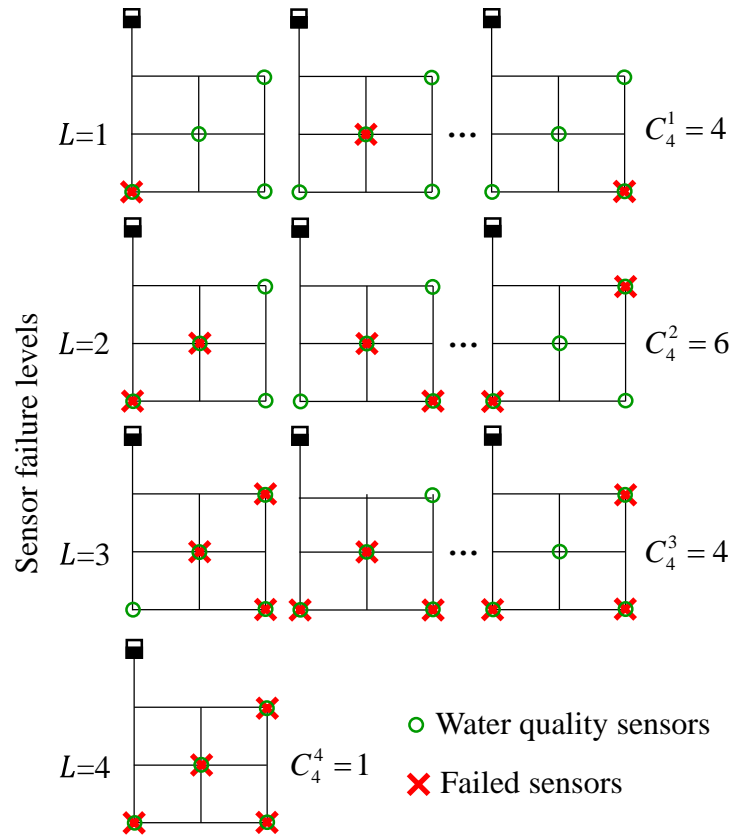


Fig. 2. A schematic of sensor failure scenarios in a simple WDS with four sensors at different failure levels (L). The total number of failure scenarios for $L=1, 2$ and 3 are $4, 6, 4$

respectively, but only three scenarios are given each of these three failure levels for illustration purpose

2.2 Resilience Assessment using EA-based optimization

2.2.1 The EA-based method to identify global resilience values

As stated in the previous section, for each failure level L , all possible failure scenarios have to be considered to enable the computation of the global resilience metrics (See Equations 4-6). However, enumerating all possible sensor failure scenarios is only applicable to WQSPS with a small number of sensors. For a relatively large WQSPS this is not tractable. For example, if WQSPS uses 30 sensors the total number of failure scenarios with $L = 1$ to 30 is 1.07×10^9 . Simulating such a large number of scenarios requires massive computational resources, which would significantly go beyond the computational budgets that are typically available in practice. Therefore, the present study develops an efficient evolutionary algorithm based method (EAM) to identify the global resilience metric values (Equations 4-6) for different sensor failure levels.

Figure 3 is used to illustrate the proposed EAM. For each given sensor failure level L , an EA is performed to identify the sensor failure scenario that has the largest detection ability of the remaining sensors of the WQSPS (Figure 3a), and the detection ability level is considered as the global resilience value R_{\max} in Equation (4). More specifically, a large number of initial solutions (sensor combinations with a given number of failed sensors L) are randomly generated, followed by solution evaluations (Equations 1-3) with the aid of EPANET2.0 as the hydraulic and water quality simulation model. These solutions are driven by the algorithm operations towards the maximum value of the detection ability levels (Figure 3a) until the final optimal solution (i.e., R_{\max}) is identified (Wu and Walski, 2006). Similarly, the EA is run again to determine the sensor

failure scenario that has the lowest detection ability level of the remaining sensors of the WQSPS (Figure 3b), which is used to represent the global resilience value R_{\min} in Equation (5). All the individual members within the entire searching of the two optimization runs are used to estimate the mean value of the detection ability levels under sensor failures ($R_{\text{mean}}(L)$ in Equation 6), as shown in Fig. 3(c).

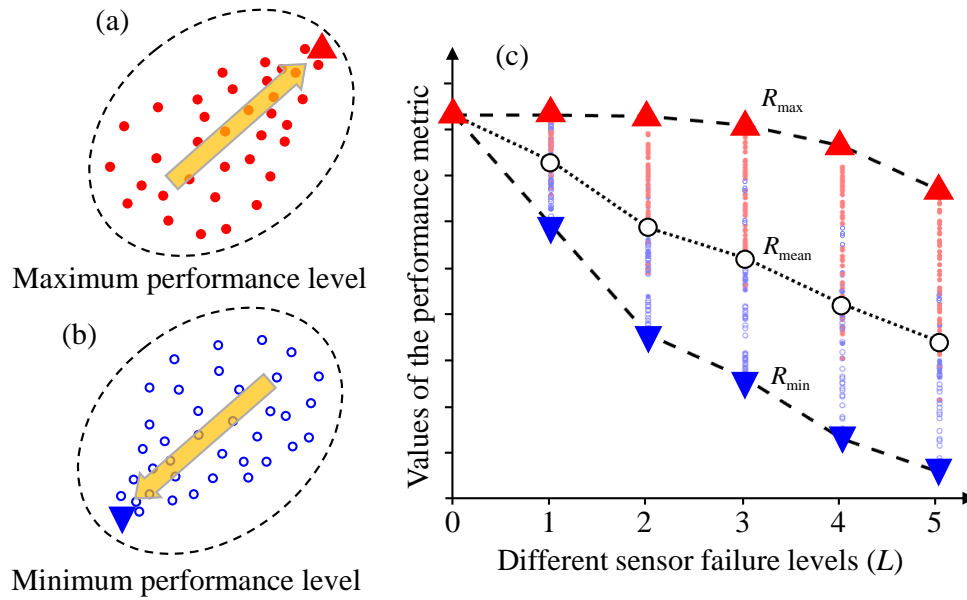


Fig. 3. Illustration of the proposed EA-based optimization method (EAM) to identify the global resilience values for different sensor failure levels (L)

2.2.2 The data-archive method to improve optimization efficiency

In the proposed method, two EA optimization runs are performed for each sensor failure level, leading to a large number of EA runs as all different failure levels have to be considered. In addition, water quality simulation models need to be frequently called to enable the performance level computation (Equations 1-3) for each EA run, which are time-consuming especially for large-scale complex WDSs. To address this issue, a new data-archive method is developed in this

288 paper to improve the computational efficiency of the optimization process. The data-archive
289 method is based on the approach described in He et al. (2018)

290 In the proposed data-archive method, a calibrated water quality model is first established,
291 followed by the specification of simulation parameters such as simulation time step and duration
292 time. Subsequently, all possible contamination scenarios (intrusion events) are defined by adding
293 a contamination source with a given injection rate and a given time period to each node
294 $i = 1, 2, \dots, N$ at different time within the total duration of a simulation described by demand
295 patterns (DP). Therefore, the total number of contamination scenarios is $N \times DP$. A water
296 quality simulation is then executed with the pre-specified parameters for each pre-defined
297 intrusion event. A data-archive is finally established to record the hydraulic and water quality
298 simulation results that are required to enable the calculation of the performance levels as a result
299 of sensor failures. However, it should be noted that the proposed data-archive approach is used to
300 reduce the need for calling a water quality simulation model for each EA function evaluation
301 conditioned on a predefined set of contamination characteristics (e.g., intrusion concentration
302 and duration). This implies that the data archive needs to be re-developed if the intrusion
303 characteristics are changed. This is a limitation of the proposed data-archive approach that needs
304 to be addressed in future. The details of the proposed method for the development of data
305 archives are shown by the pseudo-code in Figure 4 below.

Step 0: Set up the water quality simulation model for the WDS.

Step 1: Specify the simulation parameters, including the water quality time step, contamination injection quantity, injection time period, concentration threshold and total simulation duration time.

Step 2: Define all the possible contamination intrusion events for each demand node $j = 1, 2, \dots, N$ (N is the total number of demand nodes) at time $t = t_1, t_2, \dots, t_{DP}$ (DP is the length of demand pattern) as $[E_1, E_2, \dots, E_M]$ ($M = N \times DP$).

FOR $i = 1, 2, \dots, M$

Step 3: Perform the water quality simulation with the pre-specified parameters for the intrusion event E_i (the start time of the injection and which node is to be injected)

```

FOR  $m=1,2,...,TL$  ( $TL$  is the total number of sensors)
    Step 4: Perform the water quality simulation model for the intrusion event  $E_i$  with the pre-
        specified total duration time
        If  $E_i$  can be detected by the  $m^{\text{th}}$  sensor
             $T_i = t_i^d$ 
        Otherwise
             $T_i = t_i^e$ 
    FOR  $t = 0, \Delta t, 2\Delta t, ..., B\Delta t$  ( $T_i = B\Delta t$ )
        Step 5: Perform the water quality simulation model at time  $t$ , and record
             $Q_j(S_{TL-1}^m, E_i, t)$  and  $DQ_j(t)$  for each demand node  $j$ , where  $S_{TL-1}^m$  represents
            that only the  $m^{\text{th}}$  sensor is considered and the all the other sensors are failed
            (i.e., the failure level is  $TL-1$ ). This is followed by the use of Equation (1) to
            calculate and record  $FL(S_L^k, E_i, t)$  for each  $t$ .
        END  $t$ 
    Step 6: Compute  $\int_{t_i^s}^{T_i} FL(S_{TL-1}^m, E_i, t) dt$  in Equation (2), which equals to the total values of
         $FL(S_L^k, E_i, t)$  across different time.
    Step 7: Develop a data-archive for the event of  $E_i$  and the sensor  $m$ , referred to
         $\Phi(E_i, m) = \{t_i^s, t_i^e, T_i, \int_{t_i^s}^{T_i} FL(S_{TL-1}^m, E_i, t) dt\}$ 
    END  $m$ 
END  $i$ 

```

Fig. 4. The pseudo-code of the development of the data archives in the proposed method

Relative to the data-archive method stated in He et al. (2018) that only recorded the time of each sensor in detecting each of the contamination events (t_i^d), the archive structure used in this paper has been significantly extended by adding a larger number of variables including t_i^s, t_i^e, T_i , and $\int_{t_i^s}^{T_i} FL(S_{TL-1}^m, E_i, t) dt$ as shown in the pseudo-code (Figure 4). The application procedures of the developed data archives within the optimization framework are outlined in Figure 5 by pseudo codes. As shown in Figure 5, a total of Pop initial solutions is first randomly generated for each sensor failure level (L), followed by solution evaluations for all M intrusion events based on Equations 1-3. The individuals that are survived from the selection operator are

315 subject to cross and mutation operations, and the generated offspring are driven by the EA
 316 operations towards the optimal value until the final optimal solution is identified.

FOR $L=1, 2, \dots, TL$

FOR $n=1, 2, \dots, Pop$ (Pop is the population size of the evolutionary algorithm, representing a sensor failure scenario with $TL-L$ valid sensors)

FOR $i = 1, 2, \dots, M$ (M is the total number of intrusion events)

Step 1: Identify the sensor m that has the minimum value of T_i information recorded at the data archive (Φ) from all $TL-L$ valid sensors.

Step 2: Compute and record $\left[1 - \frac{1}{(t_i^e - t_i^s)} \int_{t_i^s}^{t_i^e} FL(S_L^k, E_i, t) dt \right]$ in Equation (2).

END i

Step 3: Compute and record $f(S_L^k)$ in Equation (2) using all the values recorded in Step 2.

END n

Step 4: Carry out the algorithm operators to lead the search towards identifying the minimum or maximum resilience values as defined in Equations 4 and 5. All the recorded values in Step 3 over different EA iterations are used to compute the mean of the global resilience values in Equation (6).

END L

317 **Fig. 5. The pseudo-code of the applications of the data archives in the proposed method**

318 **2.3 Sensor Ranking**

319 In the proposed method, the sensors are ranked based on their impact on the global resilience
 320 values obtained using methodology shown in the above section, thereby indicating their relative
 321 importance in affecting the performance of the WQSPS induced by their failures. More
 322 specifically, the frequency of the sensors associated with the lowest global resilience values
 323 across different failure levels is used to enable the ranking, with details represented by the two
 324 equations below,

$$P_s(i) = \frac{1}{TL} \sum_{L=1}^{TL} \gamma(i, L) \quad (7)$$

$$\gamma(i, L) = \begin{cases} 1, & \text{Sensor } i \text{ is selected} \\ 0, & \text{Otherwise} \end{cases} \quad (8)$$

where $P_s(i)$ is the probability of the sensor i that has been identified to be included in the failure scenarios associated with the lowest reliance values (R_{\min}) over all different failure levels; TL is the total number of sensors; $\gamma(i, L)$ is an indicator function, with $\gamma(i, L) = 1$ if the sensor i is in the failure scenario of R_{\min} at the failure level L , which is identified by the EA-based optimization method, otherwise $\gamma(i, L) = 0$. For example, if a sensor is selected three times in the failure scenario of R_{\min} relative to a total of six failure levels, it has a $P_s(i) = 50\%$. As shown in Equation (7), a sensor with a larger value of $P_s(i)$ indicates that this sensor is overall more important as its failure is likely to induce more serious consequences relative to the sensors with low $P_s(i)$ values. Such knowledge is practically important as it can be used as guidance for the management and maintenance of water quality sensor systems.

3. Case Studies

3.1. Description

Two real-world WDSs in China, the Jiayou network (JYN) and the Zhuohao network (ZHN), are selected as case studies to demonstrate the proposed EA-based global resilience assessment method. The JYN consists of two reservoirs, 349 demand nodes and 509 pipes with many loops (Figure 6), and The ZHN has one reservoir, 3,439 demand nodes and 3,512 pipes with many branches (Figure 7). Both WDSs have a demand pattern varying over 24 hours, with each hour

representing a demand scenario. The JYN and ZHN network supplies approximately 256,592 m³ per day and 140,782 m³ per day respectively. Six and 30 water quality sensors (He et al. 2018) are available for JYN and ZHN, respectively. Four different water quality sensor placement strategies (WQSPSs) have been identified for each case study as shown in Figures 6 and 7. These four WQSPSs were identified by He et al. (2018) who used an optimization algorithm. Different contamination probability functions were considered to enable the WQSPS optimization. More specifically, the WQSPS1, WQSPS2, WQSPS3 and WQSPS4 for both case studies were determined using the equal contamination probability function at each node, the probability function based on nodal demands, the probability function based on length of pipes immediately connected to the contaminated nodes, and the probability function based on user properties, respectively (see He et al. (2018) for details). This study aims to investigate the global resilience of the four WQSPSs with sensor failures considered, thereby facilitating the selection of the resilient sensor deployment methods.

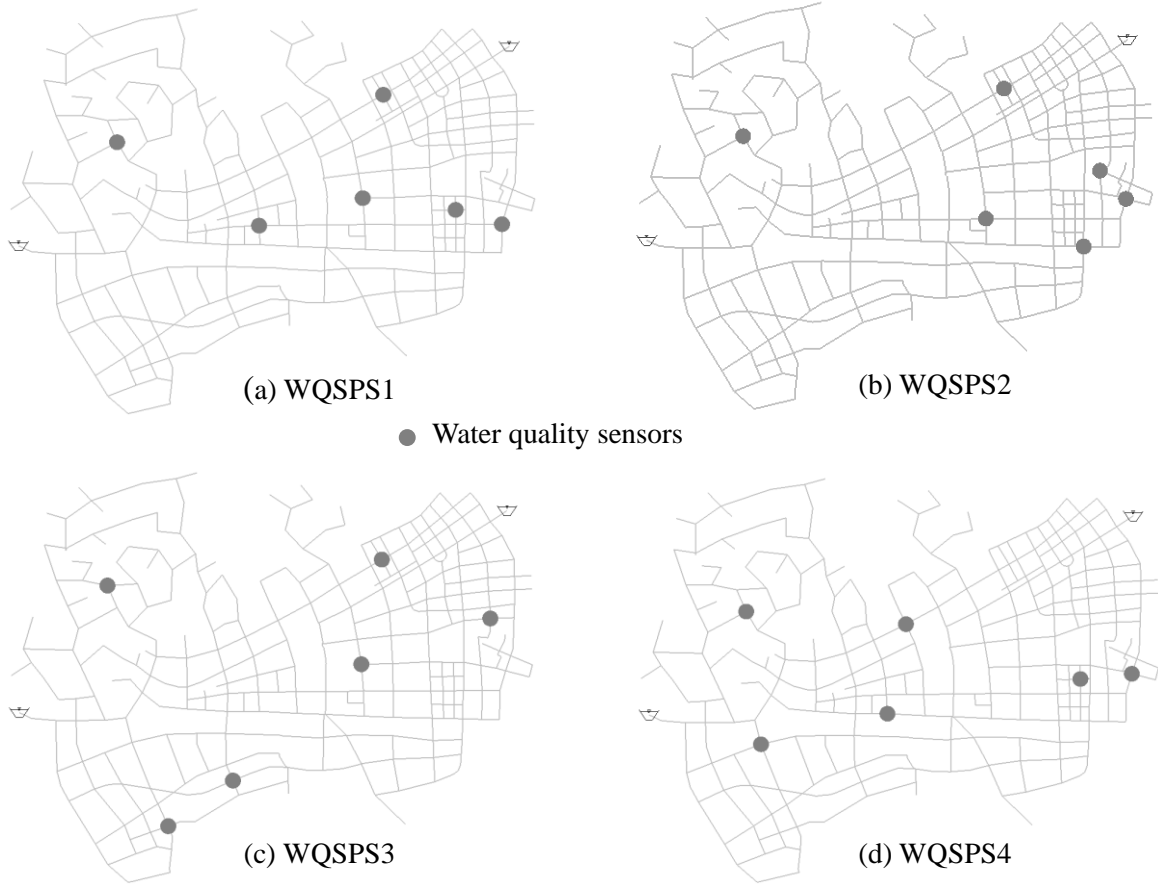


Figure 6 The network typology of the JYN case study with four water quality sensor placement strategies (WQSPSs)

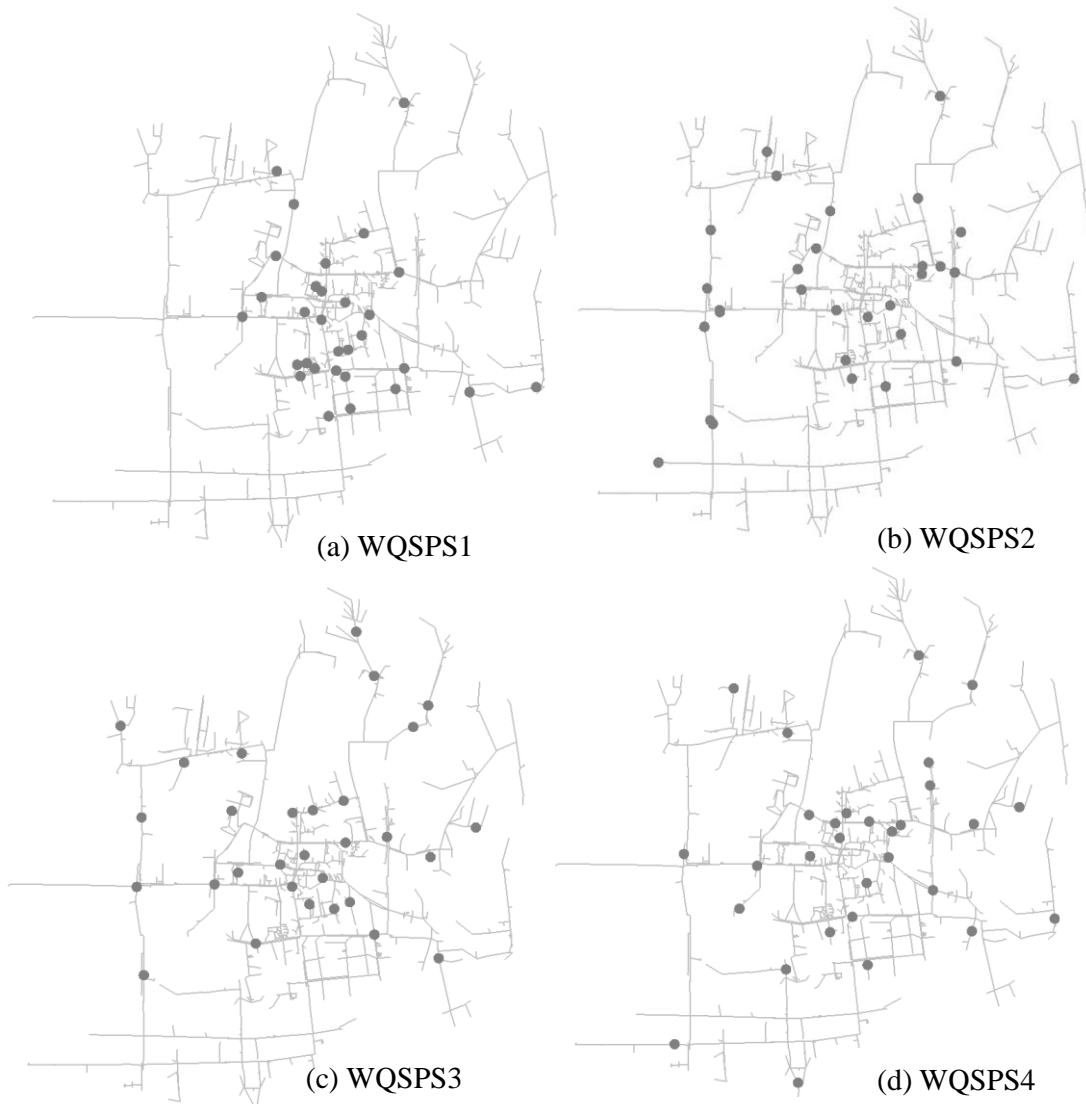


Figure 7 The network typology of the ZHN case study with four water quality sensor placement strategies (WQSPSs)

3.2 Application of the proposed method

The EPANET2.0 was used as the hydraulic and water quality simulation model in this study. For each case study, a total duration of 96 hours (four times of the 24-hour demand pattern) with a time step of 5 minutes was used to simulate each contamination scenario. Following Ostfeld et al. (2008), a contamination scenario was represented by adding a contamination source to a node

with an injection rate of 100 mg/L of two-hour duration. Consequently, the total numbers of contamination scenarios for JYN and ZHN case studies were $24 \times 349 = 8,376$ and $24 \times 3439 = 82,536$, respectively. The detection threshold of water quality sensors was set to 0.01 mg/L following He et al. (2018). It is noted that as each node of the WDS was considered as the intrusion injection location at a wide range of injection time, it is believed that the defined contamination events were representative following the description in Tinelli et al. (2017).

In the present study, the evolutionary algorithm Borg (Hadka and Reed, 2013; Zheng et al., 2016), which has been successfully and widely used to deal with various water resources optimization problems, was employed to solve the proposed optimization problem. The population size of Borg applied to JYN and ZHN case studies were 500 and 1,000 respectively following the parameters used in He et al. (2018), and the maximum allowable number of evaluations was 500,000 for both case studies. The values of the remaining parameters of Borg were the default selections in Wang et al. (2014), which have been validated and verified through various applications. Five runs of the Borg with random number seeds were applied to each case study, and the results were overall similar among different runs.

3.3 The traditional global resilience analysis (TGRA) approach

The traditional global resilience analysis (TGRA) approach has been widely used to assess the resilience of various systems as a result of malfunctions (e.g., pipe breaks), such as electrical power systems (Johansson, 2010), urban drainage systems (Mugume et al., 2015) and water distribution systems (Diao et al., 2016). To demonstrate the capacity of the proposed EA-based method, its performance is compared with the TGRA presented in Diao et al. (2016) in terms of their ability to capture the global resilience values.

The TGRA provided a response curve (envelope) that represented the range of resilience (corresponding Equations 4-6) under increasing failure levels by evaluating a limited number of failure scenarios. When only one sensor in WDS failed (i.e., the failure level $L = 1$), it required each sensor to be traversed and hence a total of M failure scenarios needed to be evaluated. When all the sensors failed ($L = TL$), there was only one failure scenario to be considered. For $1 < L < TL$, the TGRA involved two different types of failure scenario selections, which were targeted failure type and random failure type (Diao et al., 2016). The targeted failure scenarios were determined through an incremental manner, where the sensor with the largest/lowest impact on the performance of WQSPS was incrementally added to the failure scenario as the failure level increased. The random failure scenario selection aimed to enrich the targeted failure scenarios through selecting the locations of L failed sensors randomly, thereby improving the likelihood to identify the near-optimal failure scenarios that have the largest or lowest global resilience values. Details of the TGRA can be found in Mugume et al. (2015) and Diao et al (2016).

4. Results and discussions

4.1 Comparison between the proposed EAM and the TGRA

The values of the three global resilience metrics defined in Equations (4-6) were identified by the proposed EAM and the TGRA respectively, with results given in Figures 8 (JYN) and 9 (ZHN). For the JYN with a relatively small number of sensors (six), it was seen that the proposed EAM exhibited similar performance with the TGRA in terms of R_{\max} , R_{\min} and R_{mean} values for each failure level applied to the four sensor placement strategies (SPSs). To further verify the effectiveness of the proposed EAM, all the possible failure scenarios for each failure level were

410 fully enumerated to enable the identification of the global values of the global resilience metrics,
 411 with results also shown in Figure 8 (the EM). It is observed that while the R_{mean} values were
 412 slightly different between the proposed EAM and the EM, the R_{max} and R_{min} values identified by
 413 the EAM consistently matched those from the EM. This was also the case for the traditional global
 414 resilience analysis method (TGRA) as shown in Figure 8. Using the results of the JYN case study
 415 with six sensors, it can be deduced that the proposed EAM was effective in identifying the global
 416 resilience values.

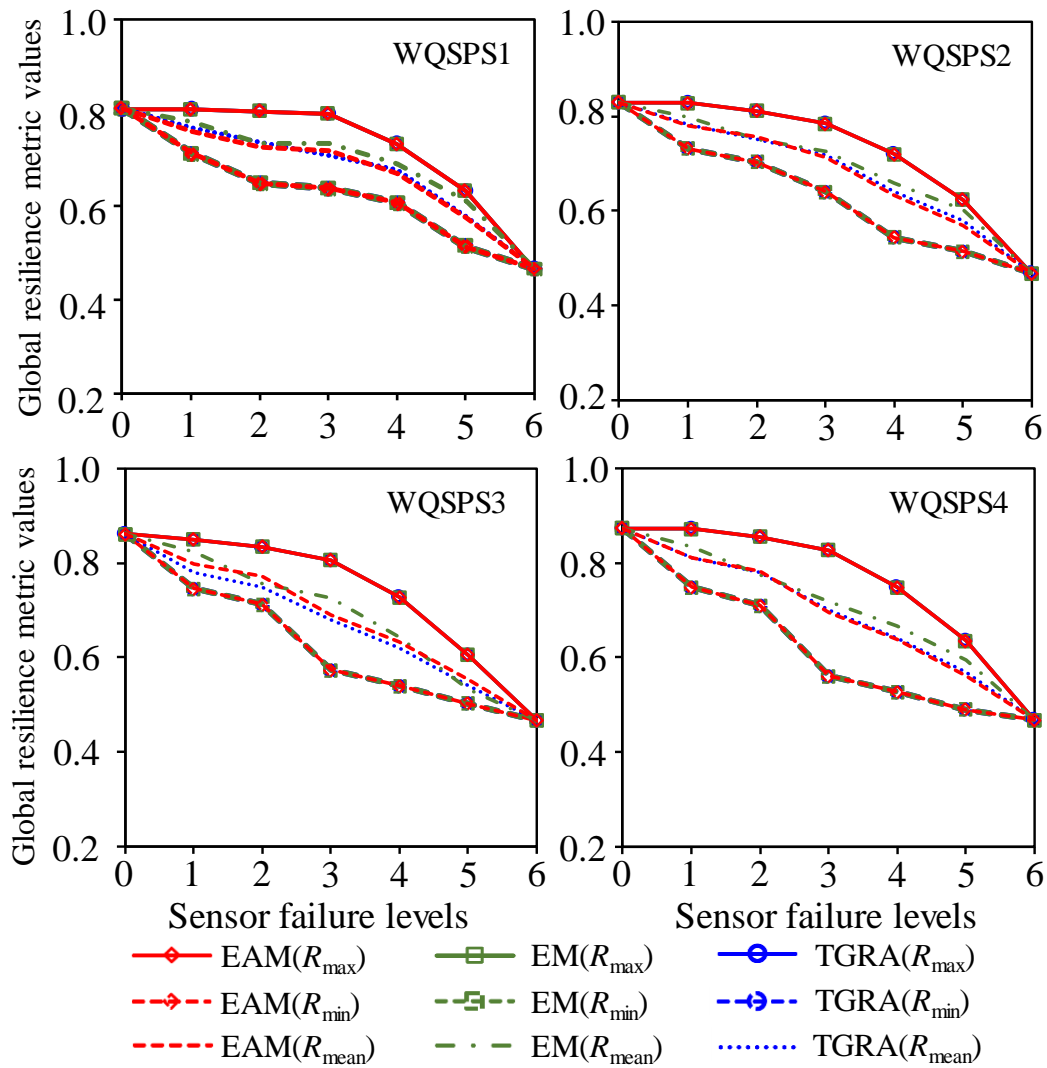


Fig. 8. Global resilience metric values of different failure levels applied to the four different WQSPSs of the JYN study

Interestingly, when the methods were applied to the ZHN with 30 sensors (Figure 9), the envelope results produced by the EAM results consistently outperformed those from the TGRA across all sensor levels. This was especially the case for the R_{\min} as the proposed EAM was able to identify sensor failure scenarios with substantially more serious impacts on the WQSPS's detection performance compared to the TGRA. For instance, if 20 sensors failed for the SPS2 (Figure 9(b)), the value of R_{\min} identified by the proposed EAM was 0.78, but the TGRA offered a value of $R_{\min}=0.84$. This indicated that the TGRA can significantly underestimate the potential impacts of sensor failures on the detection performance of the water quality sensor systems. As shown in Figure 9, the advantage of the proposed EAM relative to the TGRA became more prominent for failure levels (L) between 10-20 (i.e., the number of failed sensors were between 10 and 20) for all the four WQSPSs. This was expected as the total search space for the L between 10 and 20 was appreciably larger than other failure levels, and hence the TGRA had a lower likelihood to identify the global resilience metric values (minimum or maximum values) relative to the proposed EAM.

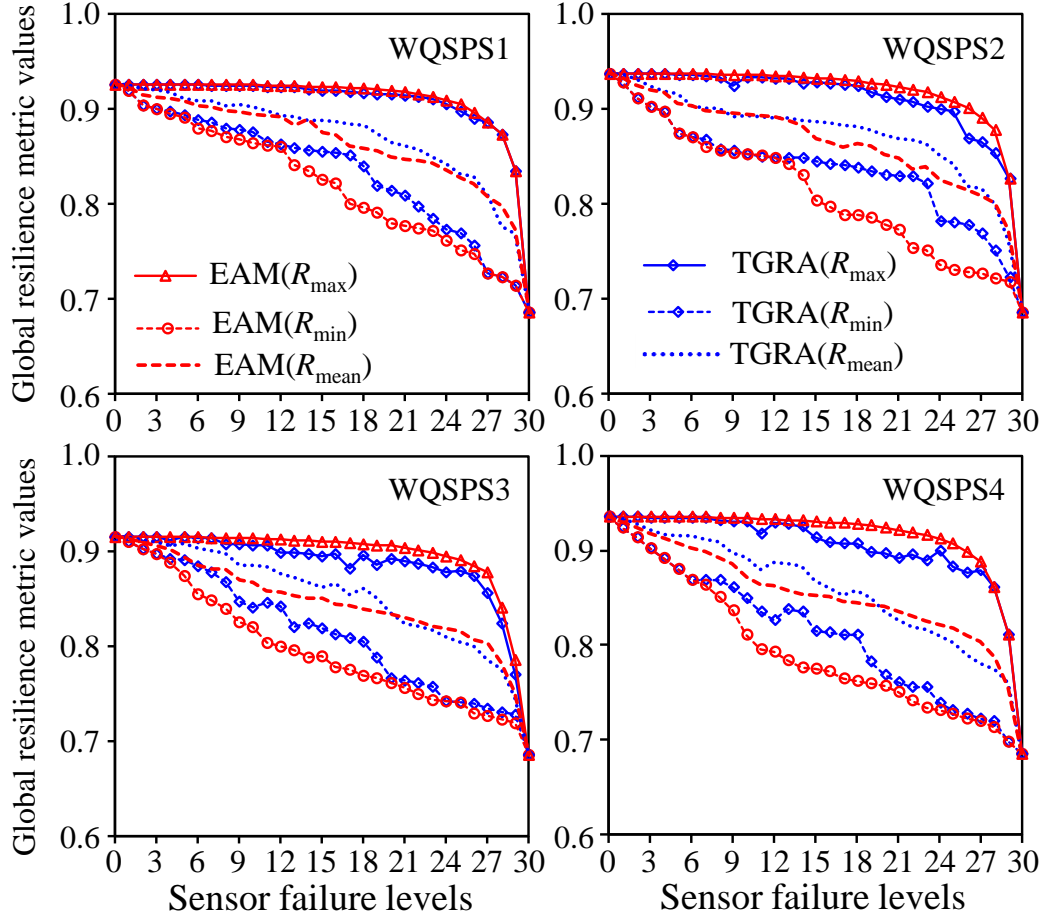


Fig. 9. Global resilience metric values of different failure levels applied to the four different WQSPSs of the ZHN case study

To reveal the underlying mechanisms that caused the performance variation between the proposed EAM and the TGRA, Figure 10 presents the locations of the failed sensors at four different failure levels (L) identified by these two methods applied to WQSPS1 of the ZHN case study based on R_{\min} metric. As shown in this figure, at $L = 3$, the locations of the three sensors with their failures having the largest impacts of the WQSPS1's detection performance were identical between these two methods (Figure 10a). However, for the EAM identified failure scenario based on R_{\min} metric when $L=4$ (Figure 10b), one sensor has been removed when

444 compared to the failure scenario with $L=3$, and two new sensors have been added to the failure
445 scenario with $L=4$. However, for the TGRA, only one more sensor has been added to its already
446 identified failure scenario based on R_{\min} metric when $L=4$. This was also the case when L
447 increased to 5 and 15 as shown in Figure 9(c,d). This was because the TGRA selected the failed
448 sensors mainly using an incremental (greedy) manner, where the sensor whose failure has the
449 largest impacts on the WQSPS's detection performance was incrementally added to the failure
450 scenario as the failure level increased. Therefore, the identified failed sensors were highly likely
451 to be trapped in a local solution. In contrast, the proposed EAM identified failed sensors
452 independently for each failure level, and hence it was able to find improved global resilience
453 metric values compared to the TGRA, especially for the large and complex problems (Figure 9).

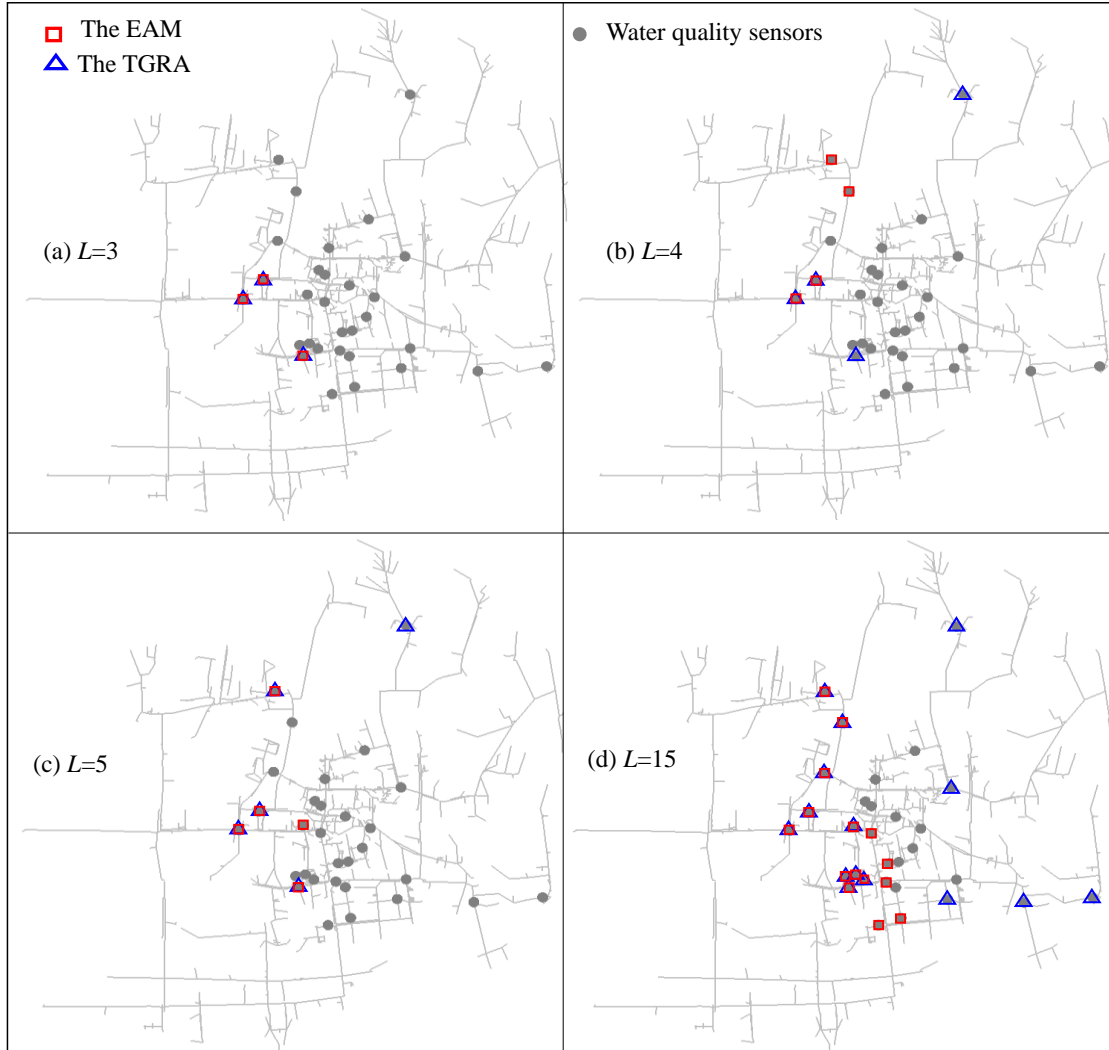


Fig. 10. Locations of sensors (to whose failure the resilience is sensitive) identified by the proposed EAM and TGRA methods applied to WQSPS1 (Figure 7) of the ZHN based on R_{\min} metric

In terms of computational analysis, the computational budgets of the proposed EAM were primarily used by the generation of data archive that involved water quality simulations. For the ZHN case study, the total number of contamination scenarios considered was the value computed by the number of nodes (3,439) multiplied with the number of demand patterns (24), leading to a total of 82,536 events. Using a PC with 4.00-GHz Intel Core i9-7980XE processor in Windows

10, the total time for simulating these events for data archive development was 19.6 hours (note that data archive only needed to be developed once). Within the optimization process, the established data archive, rather than the water quality simulator, was used to enable the objective function evaluations. Consequently, the optimization process was very efficient with a total of approximately 0.5 hours for all optimization runs. Therefore, the total computational time used to identify the global resilience metric values for the ZHN case study was 20.1 hours, which is practically affordable. For the TGRA, a total of 11,679 sensor failure scenarios was identified using the method described in Diao et al. (2016), and for each scenario, all the 82,536 contamination events had to be simulated to enable the objective function evaluations. The estimated computational time was 229,261 hours or about 9,500 days ($11,679 \times 19.6$ hours used for the simulating 82,536 contamination events), which is impossible to complete. Therefore, the established data archive was also used by the TGRA to produce the results, and hence the total computational time of the TGRA was similar to that used by the proposed EAM (the main computational budgets of each method were used by the data archive establishment). This was also the case for the small JYN case study. However, the proposed EAM can produce significantly better results for the large ZHN case study compared to the TGRA as shown in Figure 9.

4.2 Resilience comparison across different WQSPSs

Figure 11 shows the global resilience metric (R_{\min} , R_{\max} and R_{mean}) values of each WQSPS for the two case studies over all different failure levels (L). All these values were divided by R_0 (the global resilience value of WQSPS without sensor failures) to enable the performance comparison of the four WQSPSs. As shown in Figure 11, for each case study, the R_0 values were overall

similar for the four WQSPSs, implying that the difference of the detection performance of the four WQSPSs without any sensor failures was negligible.

As expected, the detection performances of the four WQSPSs were consistently reduced as measured by the three global resilience metric values when the failure level increased for both case studies. Among the four WQSPSs, the WQSPS2 had an overall greater ability in maintaining its detection performance for both case studies under different failure levels compared to its counterparts. In contrast, the WQSPS4 exhibited the worst performance for the two case studies as it consistently exhibited the fastest performance deterioration in R_{\min} and R_{mean} induced by sensor failures with different levels.

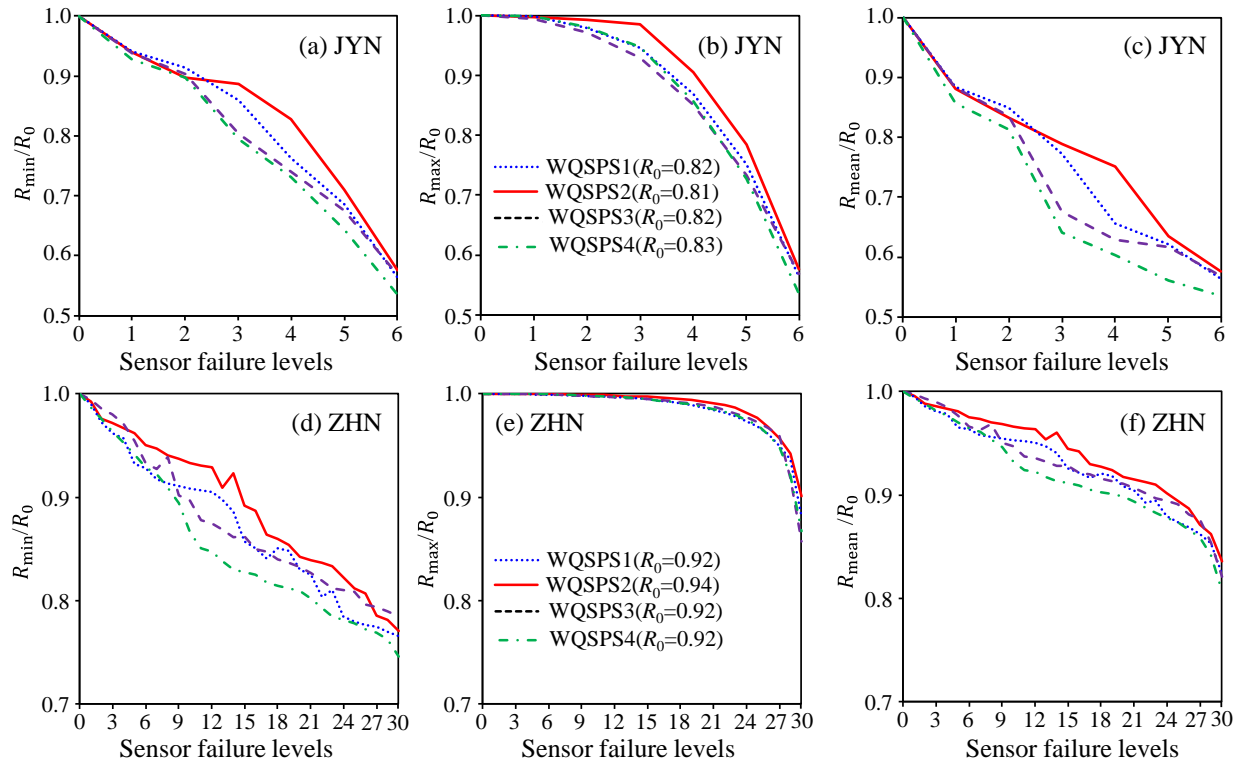


Fig. 11. Global resilience metric values of the four WQSPSs under all failure levels (L) for the two case studies (R_0 is the global resilience value of WQSPS without sensor failures)

The rationale behind the observations made above was that the WQSPS2 was identified based on deploying sensors closer to large demand users (He et al. 2018). Therefore, the contamination events at these large demand nodes that could result in large functionality losses of the WDS can be detected in an efficient manner. Consequently, this sensor deployment strategy (WQSPS2) tended to be overall more resilient as measured by the proposed global resilience metrics. While the WQSPS4 also considered the demand values within its deployment, many sensors were located exactly at the important users such as hospitals and schools as stated in He et al. (2018) (this was the main difference between WQSPS2 and WQSPS4). Consequently, the global resilience of this deployment strategy can be significantly reduced if the sensors at the important users simultaneously failed. Therefore, the WQSPS2 was identified as the most resilient system for both the JYN and ZHN case studies in dealing with sensor failures.

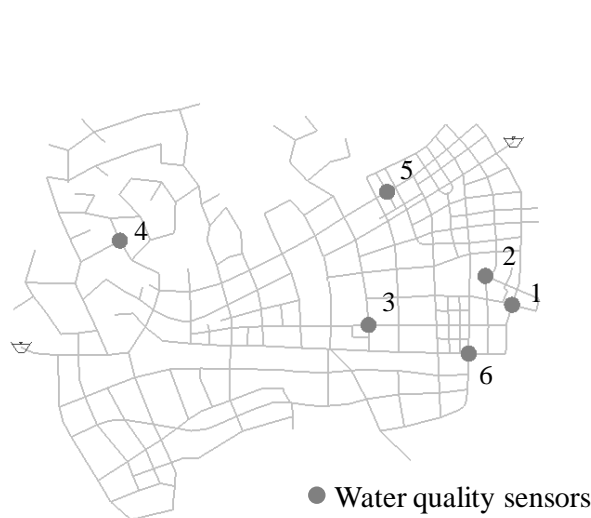
Another interesting observation from Figure 11 is that while WQSPS2 exhibited the overall best performance in global resilience metric values across different failure levels, this sensor deployment strategy performed similarly with the other three alternatives when the failure level was low, such as L between 1 and 3. This is because many contamination events can be detected by multiple sensors with relatively small time differences due to the looped water delivery manner as well as relative large sensor density (e.g., 30 sensors for the ZHN). Consequently, the relatively low sensor failure levels (e.g., $L=2$) would not induce significant variations across different WQSPSs given that their initial detection ability levels were overall similar. This implies that the global resilience that accounts for all possible failure scenarios (as it was done in this study) can provide knowledge/insights, which goes beyond the resilience analysis only considering limited failure scenarios (e.g., L between 1 and 3) as did in the majority of previous studies (Preis and Ostfeld 2008, Berry et al. 2009).

4.3 Ranking the sensors within the WQSPSs

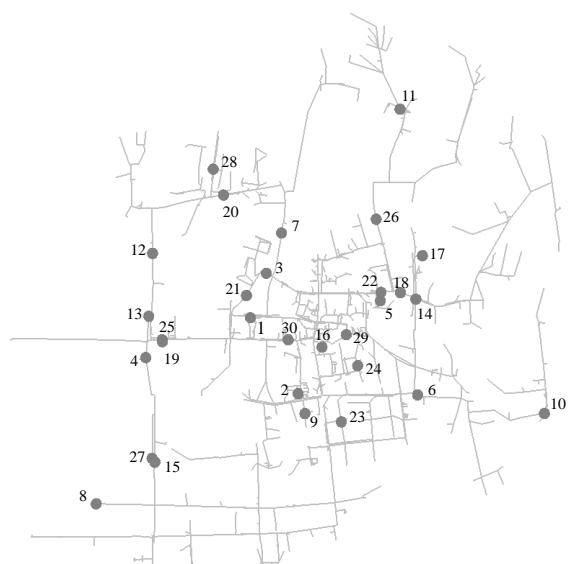
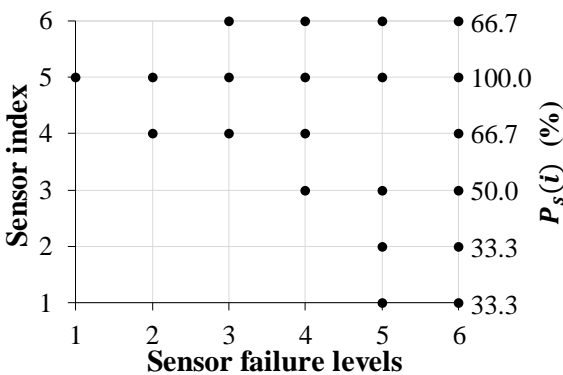
The sensors of the WQSPS2 for the JYN and the ZHN (identified as the most resilient design solutions in the previous section) were ranked based on the R_{\min} values of all different failure levels, with results given in Figure 12. It was seen that Sensor 5 was selected in all failure scenarios (100% probability to be included in the failure scenarios) associated with R_{\min} within the WQSPS2 of the JYN (Figure 12(c)), and hence this sensor was crucial in maintaining the overall detection performance of the sensor system (the locations of Sensor 5 was shown in Figure 12(a)). Sensor 4 was selected in addition to Sensor 5 as the two sensors that have the largest impact on the WQSPS2 detection performance due to their simultaneous failures, i.e., $L=2$, as shown in Figure 12(c). For the WQSPS2 of the ZHN case study (ranks of only six sensors were presented to enable clear visualization), Sensor 29 (Figure 12(b)) was the most important sensor as it was consistently selected to be included in the failure scenarios that produced R_{\min} (100% probability in Figure 12(d)). This was followed by Sensor 18 as it was always selected from $L=2$ to 30 as shown in Figure 12(d). Detailed analysis of results revealed that sensors with a relatively high rank were either located in the surrounding regions of the large/important demand users or deployed in a region with sparse sensors. For example, Sensor 8 of the ZHN case study (low ranking with a relatively low probability) was only selected when L was relatively large as shown in Figure 12(b,d). This was because this sensor was located at the downstream end of the WDS and hence the impact of its failure on the WQSPS's detection performance can be relatively small when compared to other sensors located in the middle of the WDS.

The results of the sensor rankings based on the R_{\min} are practically significant as this knowledge can be used as guidance to enable the effective water quality sensor maintenance management.

For instance, for the WQSPS2 of the JYN, Sensor 5 needed to be maintained more frequently than other sensors as its failure consistently resulted in larger performance reduction of the WQSPS over different failure levels. This was also the case for Sensor 29 within the WQSPS2 of the ZHN case study. From the practical point of view, the number of simultaneously failed sensors often ranged between 2 to 4, and for such cases, the ranking results obtained from the global resilience analysis can also inform the sensors whose failures have the largest impacts on the WQSPS's overall detection performance. For example, if $L=2$ was considered for the two case studies, Sensors 5 and 4 for the JYN and Sensors 29 and 19 for the ZHN were identified as the most important sensors that needed to be maintained in more frequently than other sensors.



(a) WQSPS2 of JYN



(b) WQSPS2 of ZHN

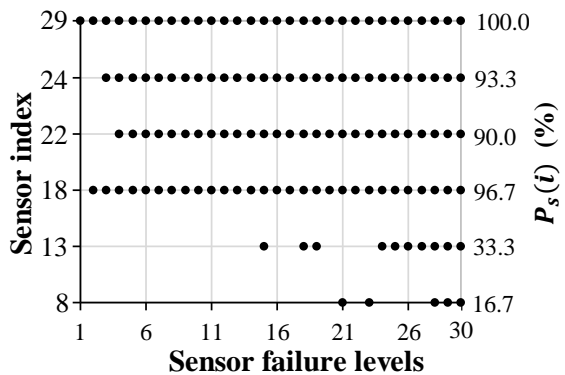


Fig. 12. Sensor rankings based on the R_{\min} of all the failure levels for both case studies,
where $P_s(i)$ is the probability of the sensor i that has been identified to be included in the
failure scenarios associated with the lowest reliance values.

4.4 Sensitivity analysis

In this section, a sensitivity analysis was conducted to evaluate the impacts of the EA runs and intrusion characteristics on the values of the global resilience metrics and sensor rankings. It is noted that the parameters of the Borg were default values based on a comprehensive sensitivity analysis performed in previous studies (Hadka and Reed, 2013; Zheng et al., 2016) and hence the parameterization strategies of Borg were not explored in this paper. This is also partly because Borg was only used as an optimization tool in the proposed method, rather than the research focus of this study. Specifically, for each case study, five different invasion scenarios were considered, which were 50 mg/L intrusion concentration with 1 hour duration, 100 mg/L intrusion concentration with 1 hour duration, 100mg/L intrusion concentration with 2 hour duration, 100 mg/L intrusion concentration with 3 hour duration, and 150 mg/L intrusion concentration with 2 hour duration. For each invasion scenario, the proposed EA-based method was run five times with different starting random seeds. Therefore, a total of 25 Borg runs were performed invasion scenario, leading to 25 global resilience metric values (R_{\max} , R_{mean} and R_{\min}) and sensor rankings over all different failure levels.

Figure 13 presents the boxplot of global resilience metric values for the large ZHN case study over all different failure levels. It can be observed from this figure that the variability of the global resilience metric values was insignificant, which was especially the case for the relatively low sensor failure levels. For instance, in terms of R_{\min} value, the largest variability occurred for

the sensor failure level $L=24$ with a maximum difference of 0.11 (from 0.69 to 0.80). Figure 14 shows the boxplot of sensor rankings based on the R_{\min} values of all the failure levels calculated from the 25 solutions for the ZHN case study. As shown in this figure, the rankings of the sensors that were associated with a high probability $P_s(i) > 80\%$ were not affected by the choices of different invasion scenarios and starting random number seeds for Borg. However, for the sensors with a moderate value of $P_s(i)$ between 40% 60%, moderate variations were observed. Similar observations were made for the small JYN case study.

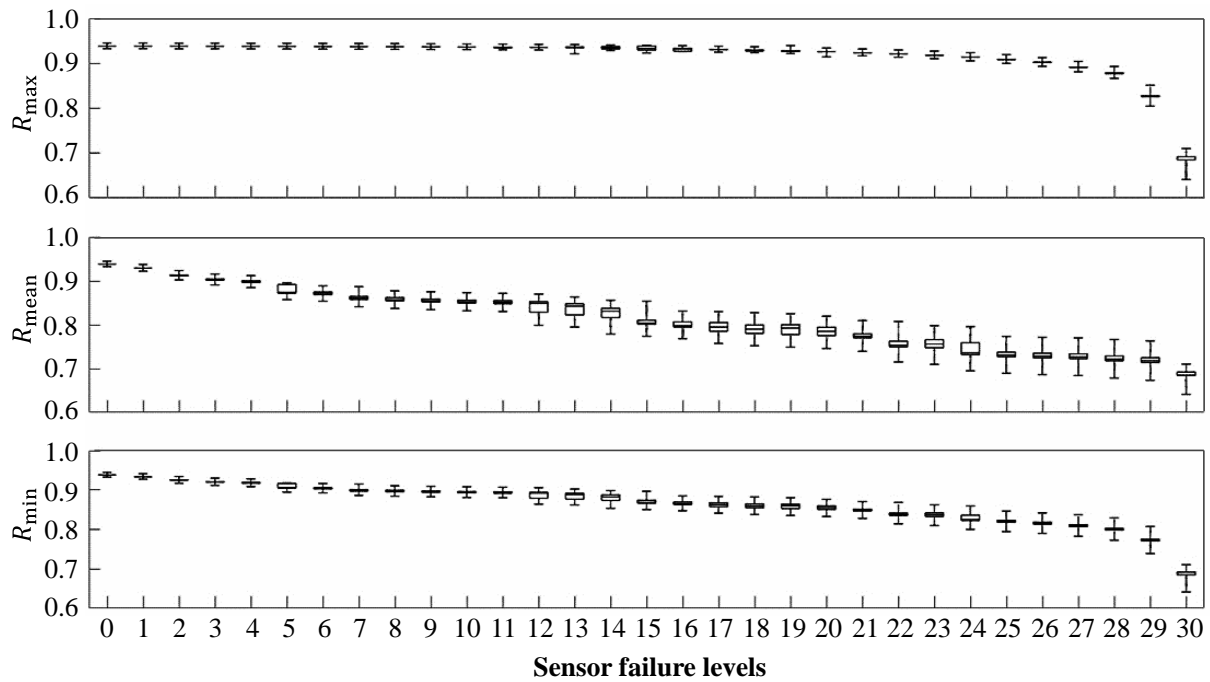


Fig. 13. Boxplot of global resilience metric (R_{\max} , R_{mean} and R_{\min}) values based on 25 Borg runs for the ZHN case study with five different invasion scenarios and five starting random number seeds over all different failure levels.

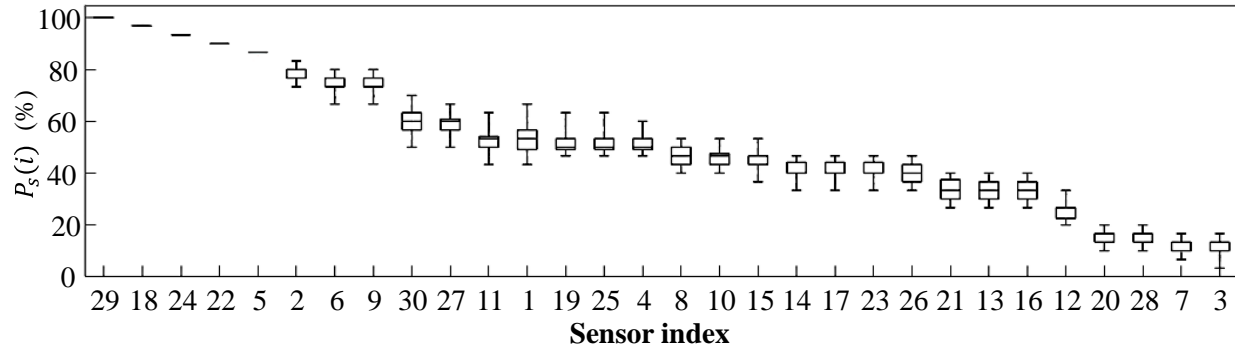


Fig. 14. Boxplot of sensor rankings based on the R_{\min} of all the failure levels calculated based on the 25 solutions for the ZHN case study, where $P_s(i)$ is the probability of the sensor i that has been identified to be included in the failure scenarios associated with the lowest reliance values

5. Summary and conclusions

A contamination early warning system is typically used to protect the water quality safety of a water distribution system (WDS), where the water quality sensors are spatially distributed to detect/warn contamination events. The majority of the current research focuses on identifying the water quality sensor placement strategy (WQSPSs) based on an assumption that all sensors are able to consistently provide accurate measurements, i.e., measure, record and communicate. However, water quality sensors are generally vulnerable to their surrounding environment and hence their failure likelihoods are often not insignificant. Therefore, it is critical to design a resilient WQSPS that cannot only detect contamination events with great effectiveness when all sensors are functioning normally, but also can maintain reasonable performance when sensors fail. However, few attempts have been made so far to explore the WQSPS's resilience

considering sensor failures, especially for the global resilience that should account for all possible failure scenarios.

This paper proposes a method to systematically assess the global resilience of WQSPSs with sensor failures considered. In the proposed method, new metrics are firstly developed to represent the global resilience of WQSPSs under different sensor failure levels (i.e., the number of simultaneously failed sensors), where all possible sensor failure scenarios are considered irrespective of their occurrence probability. Subsequently, an efficient Evolutionary Algorithm (EA) based optimization approach is proposed to effectively identify the values of the global resilience metrics for different sensor failure levels. Finally, the sensors within the WQSPS are ranked based on their global resilience values. Two real-world WDSs with four WQSPSs for each WDS analyzed are used to demonstrate the utility of the proposed global resilience identification method. Based on the results obtained the following observations/implications can be made:

- (i) The proposed EA-based optimization method (EAM) was able to identify improved values of the global resilience metrics relative to the traditional global resilience analysis (TGRA) method that has been widely used so far for the WDS with a large number of sensors (Mugume et al., 2015, Diao et al., 2016). The advantage of the proposed EAM is more prominent when dealing with WQSPSs with a large number of sensors. This implied that the TGRA results may underestimate the potentially extreme impacts/consequences of the sensor failures on the WQSPS's detection performance, and this issue has been addressed using the proposed EAM.
- (ii) It was observed that the WQSPSs designed based on deploying sensors relatively closer to large demand users (WQSPS2) were overall more resilient in dealing with sensor failures compared to other design solutions according to the definition of the global

resilience metrics (R_{mean}). However, the findings of this paper also showed that deploying sensors very close to large users or important users (e.g., hospitals or schools) can also risky as their failures can significantly reduce the detection performance of the WQSPS. These insights were practically informative as it can be used to facilitate the selection of WQSPSs for the WDS.

- (iii) The sensor ranking based on the global resilience metric values (R_{min}) can identify the important sensors whose failures would significantly reduce the WQSPS performance at different failure levels. In addition, a sensitivity analysis showed that these rankings were not significantly affected by the intrusion properties (injection concentrations and durations). Such knowledge can provide guidance to enable efficient and effective water quality sensor management as the highly ranked sensors were prioritized for maintenance due to their large impacts on WQSPS's detection performance.

It should be noted that global resilience of identified optimal WQSPSs was assessed in the current paper as suggested by previous studies (Mugume et al., 2015, Diao et al., 2016). This was done post WQSPS optimization as incorporating such a methodology directly into the optimization process would be extremely computationally expensive. It is acknowledged that assessing the global resilience of WQSPS post-optimization rather than optimizing for global resilience in the first place may result in sub-optimal solutions. Having said this, the proposed method is still of high practical significance as the identification of sub-optimal solutions using manageable computational efforts is often sufficient for real-world water resources problems (Maier et al. 2014). Still, future studies should extend the proposed method to identify the most resilient solutions considering sensor failures within the WQSPS design optimization process.

Acknowledgement

This work is funded by the National Natural Science Foundation of China (Grant No. 51922096), and Excellent Youth Natural Science Foundation of Zhejiang Province, China (LR19E080003).

References

Aral, M.M., Guan, J.B., Maslia, M.L., 2010. Optimal design of sensor placement in water distribution networks. *J. Water Resources Planning and Management* 136 (1), 5-18.

Bahadur, R., Samuels, W. B., Grayman, W., Amstutz, D., and Pickus, J. 2003. PipelineNet: A model for monitoring introduced contaminants in a distribution system. *Proc., World Water and Environmental Resources Congress 2003 and Related Symp., ASCE, Reston, Va.*

Berry, J., Carr, R. D., Hart, W. E., Leung, V. J., Phillips, C. A., and Watson, J. P. 2009. Designing contamination warning systems for municipal water networks using imperfect sensors. *J. Water Resources Planning and Management*, 135(4), 253–263.

Berry, J., Hart, W. E., Phillips, C. A., Uber, J. G., and Walski, T. M. 2005. Water quality sensor placement in water networks with budget constraints. *Proc., World Water and Environment Resources Conf., ASCE, Reston, Va.*

Bi, W., Dandy, G. C., & Maier, H. R. 2015. Improved genetic algorithm optimization of water distribution system design by incorporating domain knowledge. *Environmental Modelling & Software*, 69, 370-381.

Butler, D., Farmani, R., Fu, G., Ward, S., Diao, K., Astaraie-Imani, M. 2014. A new approach to urban water management: Safe and SuRe. In: *16th Water Distribution System Analysis*

667 Conference, WDSA. Procedia Engineering, pp. 347-354.
 668 <http://dx.doi.org/10.1016/j.proeng.2014.11.198>.

669 ChinaNews, 2016. <http://www.chinanews.com/sh/2016/05-25/7883161.shtml>.

670 Diao, K., & Rauch, W. 2013. Controllability analysis as a pre-selection method for sensor
 671 placement in water distribution systems. Water research, 47(16), 6097-6108.

672 Diao, K., C. Sweetapple, R. Farmani, G. Fu, S. Ward, and D. Butler. 2016. Global resilience
 673 analysis of water distribution systems, Water research, 106, 383-393.

674 Hart W E and Murray. R. 2010, Review of sensor placement strategies for contamination warning
 675 systems in drinking water distribution systems, Journal of Water Resources Planning and
 676 Management, 136(6), 611-619.

677 Hadka, David and Patrick Reed. 2013. Borg: An Auto-Adaptive Many-Objective Evolutionary
 678 Computing Framework. Evolutionary Computation 21, no. 2, 231-59.

679 He G, Zhang T, Zheng F, et al. 2018 An efficient multi-objective optimization method for water
 680 quality sensor placement within water distribution systems considering contamination
 681 probability variations. Water research, 143: 165-175.

682 Huang, J. J., McBean, E. A., & James, W. 2008. Multi-objective optimization for monitoring
 683 sensor placement in water distribution systems. In Water Distribution Systems Analysis
 684 Symposium 2006 (pp. 1-14).

685 Hu, C., Ren, G., Liu, C., Li, M., Jie, W. 2017. A spark-based genetic algorithm for sensor
 686 placement in large scale drinking water distribution systems. Cluster Computing. 20 (3), 1-11.

687 Johansson, J., 2010. Risk and Vulnerability Analysis of Interdependent Technical Infrastructures
688 Addressing Socio-technical Systems (PhD thesis). Lund University, Lund.

689 Kroll and King. 2010 Methods for evaluating water distribution network early warning systems.
690 Journal: American Water Works Association, 102(1), 1-11.

691 Maier, H. R., Kapelan, Z., Kasprzyk, J., Kollat, J., Matott, L. S., Cunha, M. C., Dandy, G. C.,
692 Gibbs, M. S., Keedwell, E., Marchi, A., Ostfeld, A., Savic, D., Solomatine, D. P., Vrugt, J.
693 A., Zecchin, A. C., Minsker, B. S., Barbour, E. J., Kuczera, G., Pasha, F., Castelletti, A.,
694 Giuliani, M., and Reed, P. M. (2014). "Evolutionary algorithms and other metaheuristics in
695 water resources: Current status, research challenges and future directions." *Environmental*
696 *Modelling & Software*, 62(0), 271-299.

697 Meng, F., G. Fu, R. Farmani, C. Sweetapple, and D. Butler. 2018, Topological attributes of
698 network resilience: A study in water distribution systems, *Water research*, 143, 376-386.

699 Mugume S N, G. D. E., Fu G, et al. 2015, A global analysis approach for investigating structural
700 resilience in urban drainage systems, *Water research*, 81, 15-26.

701 Olikar N, Ostfeld A. 2014. A coupled classification–evolutionary optimization model for
702 contamination event detection in water distribution systems. *Water research*, 51, 234-245.

703 Ostfeld, A., and Salomons, E. 2004. Optimal Layout of Early Warning Detection Stations for
704 Water Distribution Systems Security. *Journal of Water Resources Planning & Management*,
705 130(5), 377-385.

Ostfeld, A. et al. 2008 "The battle of the water sensor networks (BWSN): A design challenge for engineers and algorithms." *Journal of Water Resources Planning and Management* 134(6), 556-568.

Perelman, L., Ostfeld, A. 2011. Extreme impact contamination events sampling for real-sized water distribution systems. *Journal of Water Resources Planning and Management*, 138(5), 581-585.

Preis, A., and Ostfeld, A. 2008. Genetic algorithm for contaminant source characterization using imperfect sensors. *Civ. Eng. Environ. Syst.*, 25(1), 29–39.

Qi, Z., Zheng, F., Guo, D., Maier, H. R., Zhang, T., Yu, T., and Shao, Y. 2018. Better Understanding of the Capacity of Pressure Sensor Systems to Detect Pipe Burst within Water Distribution Networks. *Journal of Water Resources Planning and Management*, 144(7), 04018035.

Rathi, S., Gupta, R., 2015. A simple sensor placement approach for regular monitoring and contamination detection in water distribution networks. *KSCE Journal of Civil Engineering*. 20 (2), 1-12.

Soldevila, A., Blesa, J., Tornil-Sin, S., Fernandez-Canti, R.M., Puig, V., 2018. Sensor placement for classifier-based leak localization in water distribution networks using hybrid feature selection. *Computers & Chemical Engineering*. 108, 152e162.

Sweetapple, C., Fu, G., Farmani, R., & Butler, D. 2019. Exploring wastewater system performance under future threats: Does enhancing resilience increase sustainability?. *Water research*, 149, 448-459.

727 Tinelli, S. et al. 2017. Sampling significant contamination events for optimal sensor placement in
728 water distribution systems. *Journal of Water Resources Planning and Management*, 143, Issue
729 9, Article number 04017058.

730 Tinelli, S. et al. 2018. Impact of objective function selection on optimal placement of sensors in
731 water distribution networks. *Italian Journal of Engineering Geology and Environment*, Special
732 Issue, 2018, Pages 173-178.

733 Van Thienen, P. 2014. Alternative strategies for optimal water quality sensor placement in drinking
734 water distribution networks. *Hydroinformatics International Conference*, New York, 2014
735 <https://academicworks.cuny.edu/cgi/viewcontent.cgi?referer=&httpsredir=1>

736 Wang, Qi, Michele Guidolin, Dragan Savic, and Zoran Kapelan. 2014. Two-Objective Design of
737 Benchmark Problems of a Water Distribution System Via Moeas: Towards the Best-Known
738 Approximation of the True Pareto Front. *Journal of Water Resources Planning and*
739 *Management* 141, no. 3, 04014060.

740 Watson, J.P., Murray, R., Hart, W.E., 2009. Formulation and optimization of robust sensor
741 placement problems for drinking water contamination warning systems. *J. Infrastruct. Syst.*
742 15 (4), 330e339.

743 Weickgenannt, M., Kapelan, Z., Savic, D.A. and Blokker, M. 2010. Risk-based Sensor
744 Placement for Contaminant Detection in Water Distribution Systems, *Journal of Water*
745 *Resources Planning and Management (ASCE)*, 136(6), 629-636.

746 Wu, Z.Y., Walski, T., 2006. Multi-objective optimization of sensor placement in water distribution
747 systems. In: Proc., 8th Annual Water Distribution Systems Analysis Symp. ASCE, Reston,
748 Va.

749 Yang, X., Boccelli, D.L., 2016. Model-Based Event Detection for Contaminant Warning Systems.
750 Journal of Water Resources Planning and Management 142(11), 04016048.

751 Zhao, Y., Schwartz, R., Salomons, E., Ostfeld, A., Poor, H.V., 2016. New formulation and
752 optimization methods for water sensor placement. Environmental modelling & software 76,
753 128-136.

754 Zheng, F., Du, J., Diao, K., Zhang, T., Yu, T., and Shao, Y. 2018. Investigating Effectiveness of
755 Sensor Placement Strategies in Contamination Detection within Water Distribution Systems.
756 Journal of Water Resources Planning and Management, 144(4), 06018003.

757 Zheng, F., Zecchin, A., Maier, H., and Simpson, A. 2016. Comparison of the Searching Behavior
758 of NSGA-II, SAMODE, and Borg MOEAs Applied to Water Distribution System Design
759 Problems. Journal of Water Resources Planning and Management, 142(7), 04016017.

760 Zheng, F., Zecchin, A., Newman, J., Maier, H., and Dandy, G. 2017. An Adaptive Convergence-
761 Trajectory Controlled Ant Colony Optimization Algorithm with Application to Water
762 Distribution System Design Problems. IEEE Transactions on Evolutionary Computation,
763 21(5), 773-791.